Short communication

Determination of CO_2 convective mixing flux in saline aquifers based on the optimality

Huihai Liu[1]*, Jinhong Chen[1], Guodong Jin[2], Zuhair AlYousef[2]

[1]*Aramco Americas: Aramco Research Center-Houston, Texas 77084, USA*
[2]*EXPEC Advanced Research Center, Saudi Aramco, Dhahran 31311, Saudi Arabia*

Abstract:
When carbon dioxide is sequestrated in a saline aquifer, the dissolution of carbon dioxide plume results in density difference between the brine with dissolved carbon dioxide and the ambient brine. This causes fingering flow and transport, or convective mixing, that is the dominant mechanism for the carbon dioxide solubility trapping. This work presents the first theoretical relationship for the carbon dioxide convective mixing flux from the plume that is critical for evaluating the long-term safety of carbon dioxide storage in a saline aquifer. This new development is based on the optimality: the density-difference driven fingering flow and transport are self-organized in such a way that the downward mass transport rate of dissolved carbon dioxide is maximized. The optimality has a root in non-equilibrium thermodynamics and been successfully applied to modeling the gravitational fingering flow for soil water in the vadose zone. Our theoretical relationship is shown to be able to accurately predict the experimental results of the convective mixing flux in three-dimensional porous media that were reported by the two different research groups. The average relative error between the theoretical flux values and experimental observations is about 10% or less, while uncertainties exist in the test observations. The flux for Sleipner carbon dioxide injection site (22 kg/m^2/yr), estimated using our new relationship, is also consistent with the previous estimates in the literature, in a range between 0 and 30 kg/m^2/yr with the most likely value of 15 kg/m^2/yr, that were obtained using a complex model to analyze the field data. These comparisons support the usefulness and validity of our relationship that does not need the knowledge of individual fingers associated with the convective mixing and is easy to use in practice.

1. Introduction

Carbon dioxide (CO_2) geological sequestration in saline aquifers has been intensively studied in recent years because of their large CO_2 storage capacity (Ringrose, 2020). When the supercritical CO_2 is injected into a saline aquifer, a major portion of the injected CO_2 initially maintains a separated phase from brine. The CO_2 phase is lighter than brine and thus CO_2 plume is located on the top portion of the aquifer and contained by low permeability caprock overlying the aquifer.

Because CO_2 is soluble in brine, there is a boundary layer consisting of the dissolved CO_2 at the interface between brine and CO_2 plume (Neufeld et al., 2010; Brouzet et al., 2022). The brine with dissolved CO_2 is denser than the ambient brine

in a saline aquifer. The downward transport of the dissolved CO_2 is initially controlled by the diffusion process. Several experimental studies have indicated that the diffusion coefficient for the dissolved CO_2 is much larger than solute tracers in porous media (Karimaie and Lindeberg, 2017; Brouzet et al., 2022). This is because the diffusion of tracers is a result of molecule random motion within the pore network of the medium, while the effective diffusion of the dissolved CO_2 results from a combination of molecule random motion and pore-scale variation of fluid density related to CO_2 concentration (Liu and Dane, 1996). Thus, the growth rate of CO_2 diffusive zone is underestimated using the diffusion coefficient for tracers.

When the diffusive zone, containing denser fluid than ambient brine beneath it, reaches sufficient thickness for a given diffusion coefficient, downward transport of the denser fluid with dissolved CO_2 becomes unstable and is characterized by gravitational fingering with complex patterns. As previously indicated, the use of diffusion coefficient for tracers underestimates diffusive zone thickness for a given time. Consequently, the related predictions of the time for the fingering to occur may not be accurate. The fingering flow and transport, often called convective mixing in the literature, is the dominant mechanism for the CO_2 dissolution and mixing process in a saline aquifer because the convective mixing corresponds to a much larger mass transport rate for dissolved CO_2 than the diffusion process (Ennis-King and Paterson, 2003; Riaz et al., 2006; Kneafsey and Pruess, 2010; Neufeld et al., 2010; Mykkeltvedt and Nordbotten, 2012). The resulted CO_2 solubility trapping has several important implications for the long-term safety of the CO_2 storage. Firstly, the solubility trapping is a safe trapping mechanism for CO_2 storage. Because of the gravity, denser fluid or brine with dissolved CO_2 always goes downward until reaching the bottom of the aquifer and will never moves up. Secondly, for the given amounts of supercritical CO_2 and ambient brine, the denser fluid with dissolved CO_2 occupies smaller pore space, simply because it has a larger density than either supercritical CO_2 or ambient brine. Thus, the dissolution enhances CO_2 storage capacity for a given saline aquifer. Finally, the solubility trapping resulting from the CO_2 dissolution and mixing is the pre-request for CO_2 mineralization, the safest trapping mechanism in saline aquifers, given that the mineralization occurs only for dissolved CO_2. Based on the above discussion, accurate determination of the CO_2 convective mixing flux is critical for understanding and evaluating the long-term safety of CO_2 storage in deep saline aquifers.

This work focuses on the CO_2 convective mixing in saline aquifers. Laboratory studies have been reported in the literature on the mixing within either Hele-Shaw cells or two-dimensional porous media with experiment-setup sizes ranging from centimeters to tens centimeters (Kneafsey and Pruess, 2010; Neufeld et al., 2010; Backhaus et al., 2011; Tsai et al., 2013; Rasmusson et al., 2017; Mahmoodpour et al., 2019; Guo et al., 2021). Well defined fingering patterns were observed, and the related convective mixing fluxes were measured from these experiments. The relationships between the convective mixing flux and other related parameters, observed from these studies, can be very well represented with correlations between the two dimensionless parameters, Rayleigh number and Sherwood number (Neufeld et al., 2010; Backhaus et al., 2011; Erfani et al., 2022; Letelier et al., 2023). Rayleigh and Sherwood numbers represent time-scale ratio and mass-transport-rate ratio, respectively, between CO_2 diffusion and convection processes (Erfani et al., 2022). It is important to note that tests with Hele-Shaw cell may not be able to accurately capture fingering process in two-dimensional porous media because the former does not include the impact of the complex geometry of pore networks in porous media, although the general behavior of the fingering is consistent in the two systems (Letelier et al., 2023).

Furthermore, the experimental data from three-dimensional porous media indicate that the relationships obtained from the two-dimensional tests may not be applicable to the three-dimensional cases that are more representative of the aquifer conditions (Karimaie and Lindeberg, 2017).

Numerical simulation studies have also been reported in the literature with a focus on understanding the convective mixing process and interpreting the laboratory experimental observations (Pau et al., 2010; Fu et al., 2013; Paoli and Zonta, 2017; Wen et al., 2018; Erfani et al., 2022; Letelier et al., 2023). Very fine numerical grid systems were used in these studies to resolve individual fingers. The simulation results are generally consistent with small-scale experimental observations, while challenges in accurately duplicating the observations with numerical modeling were demonstrated by Newell et al. (2018). Results from a three-dimensional model were also found to give larger CO_2 convective mixing flux than a two-dimensional model for the given fluid and porous media properties (Pau et al., 2010; Lyu and Voskov, 2023).

While significant progresses have been made in understanding and modeling CO_2 convective mixing at small scales, important gaps exist in modeling the mixing at the field scale for practical applications. For example, applicability of the two-dimensional laboratory results to estimating field-scale convective mixing flux, as previously indicated, can be questioned because the test setup may not be representative of aquifer conditions. More experimental studies for three-dimensional porous media are highly desirable. Furthermore, the current modeling approaches to estimating CO_2 convective mixing flux, using the very fine numerical grid systems, may not be realistic for three-dimensional field-scale problems, because they are too computationally intensive in many cases. Note that the block size of a numerical grid must be much smaller than the width of individual fingers such that they can be accurately simulated by minimizing the numerical dispersion. Otherwise, the simulated fingers would not be representative of the reality. Thus, methods without the need to simulate individual fingers are desirable for determining the CO_2 convective mixing flux. This paper will present a method of this kind based on the optimality that the density-difference driven fingering flow and transport are self-organized in such a way that the downward mass transport rate of dissolved CO_2 is maximized. The rest of this communication is organized as follows. In Section 2, the optimality principle is briefly discussed to set up the stage for the theoretical development in this work and then the theoretical relationship developed between the CO_2 convective mixing flux and related aquifer and fluid properties. After that, an evaluation of the relationship with literature data is presented to demonstrate its validity and practical usefulness in Section 3. To the best of our knowledge, our relationship is the first theoretical one for the CO_2 convective mixing flux in a saline aquifer.

2. Optimality-based theoretical relationship

An optimality principle generally refers to that state of a physical process is controlled by an optimal condition subject to physical or resource constraints (Liu, 2011). Optimality has

been widely used in several areas. For example, the role of optimality principles in forming complex river network patterns has been recognized for many years in the surface hydrology community (Leopold and Langbein, 1962; Howard, 1990; Rinaldo et al., 1992; Rodriguez-Iturbe et al., 1992). Rodriguez-Iturbe et al. (1992) postulated principles of optimality in energy expenditure at both local and global scales for channel networks that are supported by field observations. On the other hand, applications of the optimality to subsurface flow and transport are very rare compared to those related to river networks, because the subsurface flow patterns are difficult to observe and characterize to motivate the related research activities on the subject (Liu, 2017).

Some inconsistency between the two widely used optimality principles, the minimization of energy expenditure rate principles (MEE) and the maximum entropy production principle (MEP), seems to exist even they have been successfully applied to ground surface river networks and Earth-atmosphere system, respectively (Liu, 2017). Under isothermal conditions, energy expenditure rate is proportional to entropy production rate, and therefore under such conditions, the MEP requires a river network to have the maximum energy expenditure rate for water flow. This directly contradicts the MEE supported by empirical data for river networks. To overcome this inconsistency, Liu (2017) proposed a thermodynamics hypothesis that "a nonlinear natural system that is not isolated and involves positive feedback tends to minimize its resistance to the flow process that is imposed by its environment". Essentially, the hypothesis indicates that for a system involving multiple flow and transport processes, the optimality is only applicable to the driven process that initializes the formation of flow structures, such as flow fingers or river networks. The hypothesis reconciles the MEE for river networks and MEP for the Earth-atmosphere system; the former corresponds to the minimum resistance to water flow (driven process) on the ground surface and latter to the minimum resistance to (or the maximum rate of) heat transport from equator region to the pole region of the Earth.

Based on the thermodynamics hypothesis, a macroscopic theory for gravitational fingering flow of soil water in the vadose zone has been developed by considering the corresponding optimality: "water flows in soils in such a manner that the generated flow patterns correspond to the minimum global flow resistance" (Liu, 2011, 2017, 2022). The key difference between the new theory and traditional ones for soil water flow is the mathematical expression for hydraulic conductivity. While the conductivity, in the traditional theories, is a function of water saturation or capillary pressure only, in the new theory it is related to both the capillary pressure and a power function of water flux that incorporates the impact of sub-grid fingering flow patterns. Excellent agreements between the theory and data obtained from both laboratory and field-scale infiltration tests have been demonstrated, while the traditional theories failed to predict these observations (Sheng et al., 2009; Liu, 2022, 2023). This highlights the usefulness of the optimality in dealing with highly non-linear processes. The same optimality principle based on the thermodynamics hypothesis will be used here for developing a theoretical re-

lationship for the CO_2 convective mixing flux. The difference between the current study with that by Liu (2017, 2022) is that we are here dealing with single-phase flow and the associated mass transport. Consequently, the mathematical framework used in this work is different from that used in Liu (2017, 2022).

Fig. 1 shows schematic diagram for the convective mixing for CO_2 sequestration in a saline aquifer. As previously indicated, at the interface between subcritical CO_2 plume and brine, brine with dissolved CO_2 is denser than the ambient brine below. This generates a complex fingering pattern of denser fluid containing dissolved CO_2. The purpose of this work is to develop a macroscopic framework that can accurately determine the CO_2 convective mixing flux without considering details of individual fingers. To do so, the convective mixing process is conceptualized using the cartoon shown in the lower part of the figure. The dense fluid moves downward under gravity through a portion of the aquifer and then the fresh brine is pushed upward through the rest portion of the aquifer. The fresh brine is mixed with the brine with dissolved CO_2 and dilutes its CO_2 concentration in the mixing zone near the interface between subcritical CO_2 plume and brine (Fig. 1). Since the details of fingering process are not known, the additional physical principle optimality is used here for determining the convective mixing flux. It is obvious that the driven process for the problem under the consideration is the mass transport of dissolved CO_2. Thus, the corresponding optimality principle, based on the thermodynamics hypothesis mentioned above, should be the minimization of the resistance to downward transport of dissolved CO_2, or the maximization of its transport rate.

Based on Darcy law, the vertical volumetric flux of fluid in fingering zone (lower part of Fig. 1) is given by:

$$q_f = -\frac{k}{\mu}\frac{\partial(\rho_f gz + p)}{\partial z} \quad (1)$$

where q (m/s) is flux (with positive direction being upward), subscript f refers to the fingering zone, k (m²) is aquifer vertical permeability, μ (Pa·s) is viscosity, ρ_f (kg/m³) is fluid density in the fingering zone, g (m/s²) is gravitational acceleration rate, z (m) is vertical coordinate (with positive direction being upward), and p (Pa) is pore pressure. Eq. (1) can be further rewritten as:

$$q_f = q_0 + u \quad (2)$$

$$q_0 = -\frac{k}{\mu}(\rho_0 g + \frac{\partial p}{\partial z}) \quad (3)$$

$$u = -\frac{k}{\mu}\Delta\rho_f g \quad (4)$$

where ρ_0 (kg/m³) is the density of the ambient brine and $\Delta\rho_f = \rho_f - \rho_0$ is the difference between the density in the fingering zone and the density of the ambient brine.

For the simplicity, we assume the viscosity of the fluid with dissolved CO_2 to be the same as that of the ambient brine, because the fluid viscosity is not sensitive to the CO_2 concentration here. The horizontal flow component in the brine phase is also considered to be small compared with vertical
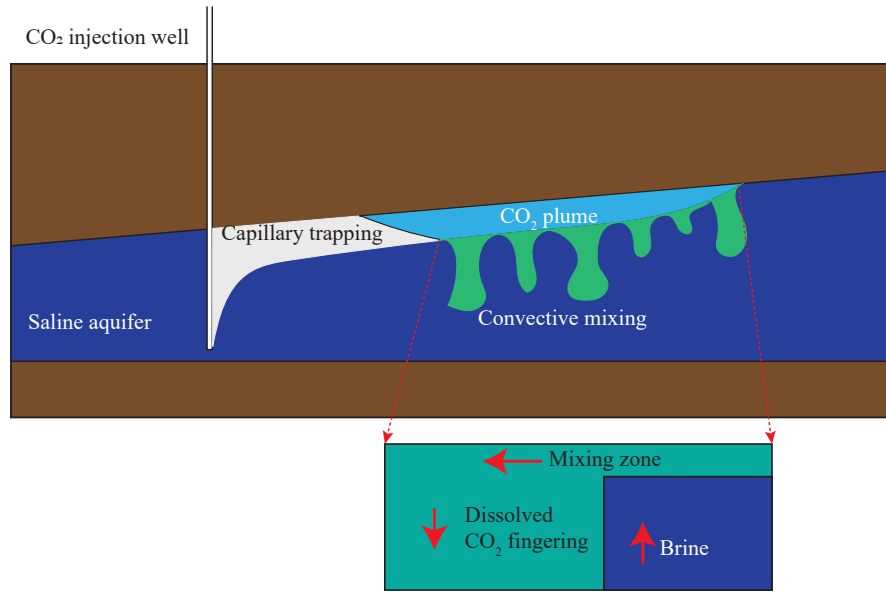
Fig. 1. Conceptualization of CO_2 convective mixing for CO_2 sequestration in a saline aquifer. The arrows (in the lower part of the figure) indicate flow directions.

fingering flow. (Note that more details on the stabilization of fingering by the horizontal flow was given by Liu and Dane (1996).) Thus, the pressures in the fingering zone and fresh brine zone are approximately the same at a given elevation within a macroscopic brine column (containing both zones) because of the negligible horizontal flow, except in the mixing zone (lower part of Fig. 1). In this case, the upward brine flux (Fig. 1) is (m/s) defined with Eq. (3).

The vertical equilibrium on the macroscopic scale is considered a good approximation for modeling CO_2 geological sequestration in saline aquifers (Celia et al., 2015). In this case, the average vertical flux within a macroscopic brine column is approximately zero, or

$$\alpha q_f + (1 - \alpha) q_0 = 0 \quad (5)$$

where α (-) is the area fraction of fingering zone on the horizontal plane within a macroscopic brine column. Alternatively, the above equation can be obtained from the volume conservation for incompressible fluids when the horizontal flow does not exist. It is easy to show that under such conditions the magnitude of downward flow rate should be equal to that of the upward flow rate at a given (macroscopic) location, which is mathematically identical to the above equation.

Combining Eqs. (2)-(5) and eliminating gives:

$$q_f = (1 - \alpha) u \quad (6)$$

Then the magnitude of mass transport flux of dissolved CO_2, resulting from convective mixing, is given by:

$$F = \alpha C_f \left| q_f \right| = (\alpha - \alpha^2) C_f \left| u \right| \quad (7)$$

where C_f (kg/m^3) is the concentration of dissolved CO_2 in the fingering zone.

Based on the optimality principle discussed above, F (kg/m^2/s) takes its maximum value for the convective mixing

process. Thus, one has

$$\frac{\partial F}{\partial \alpha} = 0 \quad (8)$$

Inserting Eq. (7) into the above equation yields:

$$\alpha = \frac{1}{2} \quad (9)$$

Note that in the derivation of Eq. (9), we consider both C_f and u to be independent of α. This is justified here, because the current study intends to develop a method for estimating convective mixing flux of dissolved CO_2 by focusing on the fingering flow just below the mixing zone (Fig. 1). In this case, lateral mixing between the fingering zone and the upward brine is not well developed yet and thus C_f and the density difference $\Delta \rho_f$ herein are approximately the same as those in the mixing zone shown in Fig. 1. Combining Eqs. (2), (7), and (9), one has

$$F = \frac{1}{4} \frac{k}{\mu} \Delta \rho_m g C_m \quad (10)$$

where subscript m refers to the mixing zone in Fig. 1.

The mixing between the dissolved CO_2 and inflowing brine in the mixing zone in Fig. 1 is a complex process. It involves dissolution from supercritical CO_2 phase, diffusion/dispersion, and the penetration of the inflowing brine into the CO_2-brine two phase flow regions (or capillary transition zone) (Neufeld et al., 2010; Elenius et al., 2014; Martinez and Hesse, 2016). Nevertheless, the dissolved CO_2 in the mixing zone ranges from the CO_2 solubility (S (kg/m^3)), at the interface between supercritical CO_2 phase and the brine phase, and zero corresponding to the inflowing fresh brine. The solubility S is the CO_2 concentration when the dissolution reaches the equilibrium. As a first-order approximation, the average CO_2 concentration within the mixing zone is determined as the average between the maximum and the minimum concentrations

in the mixing zone, or the half of S. Consequently, $\Delta\rho_m$ is approximated as the half of the difference between the fluid density ρ_s (kg/m^3), corresponding to CO_2 saturation S, and the density of ambient brine ρ_0. In this case, Eq. (10) can be written as:

$$F = \frac{K}{16}\frac{\Delta\rho}{\rho_0}S \tag{11}$$

$$\Delta\rho = \rho_s - \rho_0 \tag{12}$$

In Eq. (11), K (m/s) is aquifer's vertical hydraulic conductivity defined by:

$$K = \frac{k\rho_0 g}{\mu} \tag{13}$$

Eq. (11) is our relationship for estimating CO_2 convective mixing flux that is derived based on the optimality. While the previous studies have focused on developing the empirical relations between the flux and related aquifer and fluid properties with experimental observations (Neufeld et al., 2010; Backhaus et al., 2011; Erfani et al., 2022; Letelier et al., 2023), Eq. (11), as previously indicated, is the first theoretical relationship for the CO_2 convective mixing flux. Its usefulness will be demonstrated in the next section by comparing the theoretical calculations from the equation with the related observations of the convective mixing flux.

3. Evaluation of the relationship with data

The relationship for estimating CO_2 convective mixing flux in saline aquifers (Eq. (11)) is evaluated in this section with laboratory experiment results for three-dimensional porous media that are more representative of actual aquifer conditions than the two-dimensional porous media.

The experimental results for the three-dimensional porous media are very limited in the literature. Karimaie and Lindeberg (2017) experimentally investigated CO_2 dissolution rate induced by diffusion and convection (fingering) in a three-dimensional cell consisting of 96 µm glass beads. The permeability of 4×10^{-12} m^2 was measured with water flooding. Values of the other related parameters are provided in their Table 2 by Karimaie and Lindeberg (2017): $\mu = 1.001 \times 10^{-3}$ Pa·s; $S = 65.36$ kg/m^3, and $\Delta\rho = 12.63$ kg/m^3. In the closed testing cell, the glass beads were saturated with water and CO_2 was injected into the top part of the cell above the packed glass beads. The test was conducted under the room temperature (20°C) and the CO_2 pressure in the cell was maintained by a CO_2 pump to be a constant (60 bar). Then based on the mass balance, the CO_2 flow rate from the pump to the cell is equal to the dissolution rate and was monitored as a function of time. It was found that the dissolution rate was initially controlled by the diffusion process and then dominated by the convection. For the same experimental setup and porous media, three tests were conducted. Observed values for the convection-induced dissolution flux, or the convective mixing flux, are 1.3×10^{-6}, 2.8×10^{-6} and 1.9×10^{-6} kg/m^2/s), respectively, for the three tests. The variation in the observations reflects the challenges in accurately measuring the flux resulting from the unstable fingering flow process. In this case, the averaged

flux value (2.0×10^{-6} kg/m^2/s)) is used for evaluating Eq. (11) to minimize the observation uncertainties. The theoretical value of the CO_2 convective mixing flux, obtained with Eq. (11) and reported parameter values for the tests, is the same as the averaged observation (2.0×10^{-6} kg/m^2/s)). As indicated by Karimaie and Lindeberg (2017), the observed flux value was significantly underestimated by some commonly used empirical relations available in the literature.

Wang et al. (2016) reported an experimental study on convective mixing in three-dimensional porous media under the room temperature. In their experiment setup, melamine resin particles with different average diameters (780 and 975 µm) were packed in an acrylic resin tube with an inner diameter of 70 mm. Permeability values for these two media were measured using water flooding tests. The porous media were saturated with NaCl solution, and the top portion of the media is occupied by the denser MEG-Nal solution. Then the convective mixing flux was monitored, and three-dimensional structures of fingers imaged with X-ray computed tomography for 6 tests with different combinations of the resin particle size and fluid density difference between MEG-Nal and NaCl solutions. The experimental data were very well captured by their Eq. (11) in Wang et al. (2016) that can be rewritten as:

$$\frac{F\rho_0}{KS\Delta\rho} = 0.13Ra^{-0.07} \tag{14}$$

where Ra (-) is Rayleigh number that is between 2,600 and 9,290 for the relevant tests in Wang et al. (2016). Using the above two limits of Rayleigh number in Eq. (14), one has

$$\frac{F\rho_0}{KS\Delta\rho} = 0.068 \text{ to } 0.075 \tag{15}$$

From Eq. (11), our theoretical value for $(F\rho_0)/(KS\Delta\rho)$ is 1/16 or 0.063; the average relative error between the theoretical value and experimental observations shown in Eq. (15) is about 10%. The theoretical result is considered to be in a good agreement with experimental results, given the existence of uncertainties in the test observations.

Our theoretical prediction of CO_2 convective mixing flux is also compared with the estimation by Mykkeltvedt and Nordbotten (2012) for the well-known Sleipner CO_2 injection site. They developed a field-scale model for the CO_2 injection site with the CO_2 convective mixing flux as a fitting parameter. The model incorporated available geometric and petrophysical properties and was used for analyzing the gravimetric data that was collected for determining the CO_2 phase distribution at the injection site. Recognizing the uncertainties associated with the model input data, Mykkeltvedt and Nordbotten (2012) also conducted sensitivity studies related to the most uncertain parameters with their model. Based on the analysis of the gravimetric data and results of the sensitivity study, they concluded that the CO_2 convective mixing flux for Sleipner injection site is between 0 and 30 kg/m^2/yr (or 9.5×10^{-7} kg/m^2/s), with the most likely value being 15 kg/m^2/yr (or 4.8×10^{-7} kg/m^2/s).

To estimate the flux with our Eq. (11), the Sleipner data available in the literature is used. According to Mykkeltvedt and Nordbotten (2012), the permeability ranges from 1.0 ×

10^{-12} to 3.0×10^{-12} m^2, brine density is 1,020 kg/m^3, and the CO$_2$ mass fraction in brine (corresponding to the solubility) is 0.02. In our calculation, we used the averaged permeability of 2.0×10^{-12} m^2. There is some uncertainty in the CO$_2$ mass fraction at the Sleipner site; Audigane et al. (2006) reported the mass fraction to be 0.052, rather than 0.020. Again, we here used the average mass fraction of 0.036 corresponding to the CO$_2$ solubility (S) of 37.8 kg/m^3 that is obtained by multiplying the mass fraction with the brine density. Based on the relation between $\Delta\rho$ and S for a typical deep saline aquifer (Singh and Islam, 2018), $\Delta\rho = 0.26S = 9.8$ kg/m^3. The typical viscosity value for brine in the aquifer is $\mu = 5.9 \times 10^{-4}$ Pa·s (Neufeld et al., 2010). With these parameter values, our estimated CO$_2$ convective mixing flux at Sleipner is 22 kg/m^2/yr (or 7.0×10^{-7} kg/m^2/s). Given the considerable degree of uncertainties of the data, our theoretical result is considered consistent with the estimates obtained by Mykkeltvedt and Nordbotten (2012) using a much more complex approach and data analysis procedure.

In summary, our theoretical relationship for the CO$_2$ convective mixing flux accurately predicts the flux values observed in laboratory for three-dimensional porous media that were reported by two different groups. However, the experiment data for three-dimensional porous media are very limited at this stage; more laboratory studies of this kind, as previously indicated, are desirable for further improving our understanding of the convective mixing and evaluating the theoretical relationship. The flux for Sleipner estimated with our relationship is also consistent with the results obtained by Mykkeltvedt and Nordbotten (2012) using field data and model studies. All these clearly support the validity of our theoretical relationship that is easy to use in practice for determining the CO$_2$ convective mixing flux in saline aquifers.

4. Conclusions

This work presents the first theoretical relationship of the CO$_2$ convective mixing flux for CO$_2$ sequestration in saline aquifers. It is developed based on the optimality: the density-difference driven fingering flow and transport are self-organized in such a way that the downward mass transport rate of dissolved CO$_2$ is maximized. The relationship is shown to give the accurate predictions of the convective mixing flux values observed by different research groups from laboratory experiments using three-dimensional porous media. The flux for Sleipner estimated with our relationship is also consistent with the previous estimates from the literature that were obtained using field data and complex model analyses. These comparisons support the usefulness and validity of the developed theoretical relationship that does not need the knowledge of individual fingers associated with the convective mixing and thus is easy to use in practice.

Conflict of interest

The authors declare no competing interest.

References

Audigane, P., Gaus, I., Pruess, K., et al. A long term 2D vertical modelling study of CO$_2$ storage at Sleipner (North Sea) using TOUGHREACT. Paper Presented at Proceedings of TOUGH Symposium, Berkeley, California, 15-17 May, 2006.

Backhaus, S., Turitsyn, K., Ecke, R.E. Convective instability and mass transport of diffusion layers in a Hele-Shaw geometry. Physical Review Letters, 2011, 106: 104501.

Brouzet, C., Meheust, Y., Meunier, P. CO$_2$ convective dissolution in a three-dimensional granular porous medium: An experimental study. Physical Review Fluids, 2022, 7(3): 033802.

Celia, M. A., Bachu, S., Nordbotten, J. M., et al. Status of CO$_2$ storage in deep saline aquifers with emphasis on modeling approaches and practical simulations. Water Resources Research, 2015, 51(9): 6846-6892.

Elenius, M. T., Nordbotten, J. M., Kalisch, H. Convectivemixing influenced by the capillary transition zone. Computational Geosciences, 2014, 18: 417-431.

Ennis-King, J., Paterson, L. Role of convective mixing in the long-term storage of carbon dioxide in deep saline formations. Paper SPE 84344 Presented at the SPE Annual Technical Conference and Exhibition, Denver, Colorado, 5-8 October, 2003.

Erfani, H., Babaei, M., Berg, C. F., et al. Scaling CO$_2$ convection in confined aquifers: Effects of dispersion, permeability anisotropy and geochemistry. Advances in Water Resources, 2022, 164: 104191.

Fu, X., Cueto-Felgueroso, L., Juanes, R. Pattern formation and coarsening dynamics in three-dimensional convective mixing in porous media. Philosophical Transactions of the Royal Society A: Mathematical, Physical and Engineering Sciences, 2013, 371(2004): 20120355.

Guo, R., Sun, H., Zhao, Q., et al. A novel experimental study on density-driven instability and convective dissolution in porous media. Geophysical Research Letters, 2021, 48: e2021GL095619.

Howard, A. D. Theoretical model of optimal drainage networks. Water Resources Research, 1990, 26: 2107-2117.

Karimaie, H., Lindeberg, E. Experimental verification of CO$_2$ dissolution rate due to diffusion induced convection. Energy Procedia, 2017, 114: 4917-4925.

Kneafsey, T. J., Pruess, K. Laboratory flow experiments for visualizing carbon dioxide-induced, density-driven convection. Transport in Porous Media, 2010, 82: 123-139.

Leopold, L.B., Langbein, W. B. The concept of entropy in landscape evolution. Professional Paper, 1962: A1-A20.

Letelier, J. A., Ulloa, H. N., Leyrer, J., et al. Scaling CO$_2$-brine mixing in permeable media via analogue models. Journal of Fluid Mechanics, 2023, 962: A8.

Liu, H, Dane, J. H. A criterion for gravitational instability in miscible dense plumes. Journal of Contaminant Hydrology, 1996, 23: 233-243.

Liu, H. A conductivity relationship for steady-state unsat-

urated flow processes under optimal flow conditions. Vadose Zone Journal, 2011, 10: 736-740.

Liu, H. Fluid Flow in the Subsurface: History, Generalization and Applications of Physical Laws. Cham, Switzerland, Springer, 2017.

Liu, H. The large-scale hydraulic conductivity for gravitational fingering flow in unsaturated homogenous porous media: A review and further discussion. Water, 2022, 14: 3660.

Liu, Y., Zhang, S., Liu, H. The relationship between fingering flow fraction and water flux in unsaturated soil at the laboratory scale. Journal of Hydrology, 2023, 622: 129695.

Lyu, X., Voskov, D. Advanced modeling of enhanced CO_2 dissolution trapping in saline aquifers. International Journal of Greenhouse Gas Control, 2023, 127: 103907.

Mahmoodpour, S., Rostami, B., Soltanian, M. R., et al. Convective dissolution of carbon dioxide in deep saline aquifers: Insights from engineering a high-pressure porous visual cell. Physical Review Applied, 2019, 12(3): 034016.

Martinez, M. J., Hesse, M. A. Two-phase convective CO_2 dissolution in saline aquifers. Water Resources Research, 2016, 52: 585-599.

Mykkeltvedt, T. S., Nordbotten, J. M. Estimating effective rates of convective mixing from commercial-scale injection. Environmental Earth Sciences, 2012, 67: 527-535.

Neufeld, J. A., Hess, M. A., Riaz, A., et al. Convective dissolution of carbon dioxide in saline aquifers. Geophysical Research Letters, 2010, 17: L22404.

Newell, D. L., Carey, J. W., Backhaus, S. N., et al. Experimental study of gravitational mixing of supercritical CO_2. International Journal of Greenhouse Gas Control, 2018, 71: 62-73.

Paoli, M. D., Zonta, F. Dissolution in anisotropic porous media: Modelling convection regimes from onset to shutdown. Physics of Fluids, 2017, 29: 026601.

Pau, G. S. H., Bell, J. B., Pruess, K., et al. High-resolution simulation and characterization of density-driven flow in CO_2 storage in saline aquifers. Advances in Water Resources, 2010, 33: 443-455.

Rasmusson, M., Fagerlund, F., Rasmusson, K., et al. Tsang, refractive light-transmission technique applied to density-driven convective mixing in porous media with implications for geological CO_2 storage. Water Resources Research, 2017, 53: 8760-8780.

Riaz, A., Hesse, M., Tchelepi, H. A., et al. Onset of convection in a gravitationally unstable diffusive boundary layer in porous media. Journal of Fluid Mechanics, 2006, 548: 87-111.

Rinaldo, A., Rodriguez-Iturbe, I., Rigon, R., et al. Minimum energy and fractal structures of drainage networks. Water Resources Research, 1992, 28: 2183-2191.

Ringrose, P. How to Store CO_2 Underground: Insights from Early-Mover CCS Projects. Gewerbestrasse, Switzerland, Springer Nature, 2020.

Rodriguez-Iturbe, I., Rinaldo, A., Rigon, A., et al. Energy dissipation, runoff production and the three-dimensional structure of river basins. Water Resources Research, 1992, 28: 1095-1103.

Sheng, F., Wang, K., Zhang, R., et al. Characterizing soil preferential flow using iodine-starch staining experiments and the active region model. Journal of Hydrology, 2009, 367: 115-124.

Singh, H., Islam, A. Enhanced safety of geologic CO_2 storage with nanoparticles. International Journal of Heat and Mass Transfer, 2018, 121: 463-476.

Tsai, P. A., Riesing, K., Stone, H. A. Density-driven convection enhanced by an inclined boundary: Implications for geological CO_2 storage. Physical review E, 2013, 87(1): 011003.

Wang, L., Nakanishi, Y., Hyodo, A., et al. Three-dimensional structure of natural convection in a porous medium: Effect of dispersion on finger structure. International Journal of Greenhouse Gas Control, 2016, 53: 274-283.

Wen, B., Chang, K., Hesse, M. A. Rayleigh-darcy convection with hydrodynamic dispersion. Physical Review Fluids, 2018, 3: 123801.